

Pretransitional effects in a mesogenic mixture under an electric field

Mateusz Mrukiewicz,^{1,*} Paweł Perkowski,¹ Olga Strzeżysz,² Dorota Węglowska,² and Wiktor Piecek¹

¹*Institute of Applied Physics, Military University of Technology, 2 Urbanowicza, 00-908 Warsaw, Poland*

²*Institute of Chemistry, Military University of Technology, 2 Urbanowicza, 00-908 Warsaw, Poland*



(Received 18 October 2017; revised manuscript received 28 February 2018; published 18 May 2018)

Nematogenic liquids are materials that are in high demand for many application purposes. Field-induced nematic order in isotropic liquids can be observed by the enhancement of electric permittivity during dielectric spectroscopy measurements under the bias electric field. For this reason, dielectric measurements were done on a nematogenic mixture of highly polar compounds. This paper presents a discussion on the influence of the bias electric field on the dielectric response. We observed a decrease of electric permittivity in the isotropic phase under the bias electric field. This effect is most likely caused by the field-induced creation of some complex molecular objects. In the paper, relaxation parameters of the molecular modes were analyzed. The field-induced orientational order was determined using a dichroic ratio in a guest-host system. The measurements show the significant order parameter in the isotropic phase under an electric field.

DOI: [10.1103/PhysRevE.97.052704](https://doi.org/10.1103/PhysRevE.97.052704)

I. INTRODUCTION

In thermotropic liquid crystals, a phase sequence is controlled by temperature. In the case of nematogenic liquids, the material exhibits an isotropic phase with no orientational order in the high-temperature region, while at low temperature, the material changes to a nematic phase. The transition occurs at a specified temperature called the isotropic-nematic (*I-N*) phase transition temperature T_{I-N} or a “clearing point.” Specifically, above T_{I-N} , a nematic order exists in a small volume [1]. The short-range orientational nematic order occurs in the form of nematiclike domains [2,3]. This phenomenon is known as the pretransitional effect [4–9]. The nematic order increases as the temperature decreases toward the clearing point [10]. The sizes of domains become larger and larger. In the absence of an electric field, the direction of these domains is random. Thus, the order parameter S , which describes a degree of molecular ordering, is still equal to zero. Hence, in an isotropic material, we do not observe the birefringence effect or any other anisotropy effects. After applying an electric field, the electric birefringence effect appears because the order parameter increases. At the same time, an optical axis becomes parallel to a vector of the electric field. De Gennes, based on the Landau model [11,12], theoretically discusses the effect of the short-range nematic order in the isotropic phase affected by the electric field. This effect is enhanced close to the phase transition temperature since the director \mathbf{n} , which is parallel to the average molecular direction, has a strong tendency to align along the vector of the external electric field [11,13]. The field-induced increase of the order parameter S can be observed in the electro-optic Kerr effect experiment [14] through measuring of the induced birefringence $\delta n(E)$. Moreover, the effect is manifested apparently during

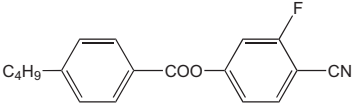
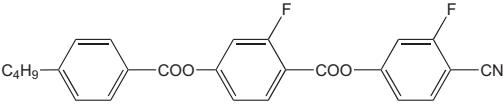
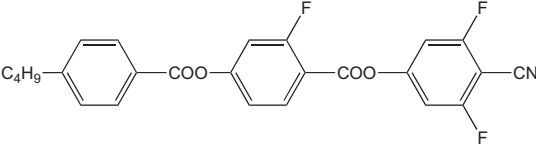
dielectric spectroscopy investigations by observation of an electric permittivity ε modulation under the bias electric field.

In this paper, we present precise dielectric spectroscopy studies about the influence of an electric field on the isotropic-nematic phase transition of a highly polar mixture. In general, electric permittivity in the isotropic phase of a typical rodlike liquid crystal material is rather constant. However, accurate measurements [15] show that electric permittivity in the isotropic phase increases slightly as temperature decreases due to an increase in the medium’s density. Therefore, electric anisotropy in the isotropic phase $\Delta\varepsilon_I$, defined as a difference between electric permittivity measured with the bias field, ε_{dc} , and without, ε_I , is zero. The situation changes when the bias electric field is applied to the highly polar mixture [16]. We observe an increase of electric permittivity in the isotropic phase, because of the creation of the short-range nematic order. As a result, the anisotropy of electric permittivity $\Delta\varepsilon_I$ becomes measurable and higher than zero, $\Delta\varepsilon_I > 0$. In the case of the nematic phase, the bias field causes the uniform orientation of the director \mathbf{n} ; thereupon the electric permittivity tensor $\hat{\varepsilon}$ is characterized with two electric parameters ε_{\perp} and ε_{\parallel} , where ε_{\perp} is electric permittivity measured in perpendicular while ε_{\parallel} is measured in parallel to the director \mathbf{n} . In the nematic phase, electric anisotropy is defined as a difference between ε_{\parallel} and ε_{\perp} ($\Delta\varepsilon = \varepsilon_{\parallel} - \varepsilon_{\perp}$).

We expect that the strong modulation of electric permittivity in the isotropic phase will be observed in liquid crystal materials with large pretransitional effects. The effects have been previously reported for rodlike, single-compound liquid crystal materials exhibiting a permanent molecular electric dipole moment μ_{\parallel} parallel to the long molecular axis [4,6,7,17–21]. Thus, we can expect in these materials a large enhancement of electric permittivity and a high value of $\Delta\varepsilon_I$ after applying the bias electric field. Under these circumstances, we created a nematogenic mixture of highly polar (NMHP) compounds which are compounds that exhibit large longitudinal dipole moments. Due to application purposes for the Kerr effect,

*Corresponding author: mateusz.mrukiewicz@wat.edu.pl

TABLE I. Molecular structure and phase transitions temperatures of components and their concentration in the NMHP mixture.

Acronym	Molecular structure	Weight percent of the compound in the mixture (%)
C1	 Cry (<i>N</i> 6.8 °C) 14.0 °C <i>I</i>	92.15
C2	 Cry 105.3 °C <i>N</i> 200.4 °C <i>I</i>	5.15
C3	 Cry 115.0 °C SmC 137.1 °C <i>N</i> 175.7 °C <i>I</i>	2.70

we aimed to obtain NMHP with a phase transition from the nematic to the isotropic phase at a low range of room temperature.

This paper presents a discussion on the possible creation of complex molecular objects forced by an electric field. These dielectric studies on molecular relaxation processes were performed in the vicinity of isotropic and nematic phase transitions. In the experiment, a field-induced order parameter was also determined using the guest-host effect [22–24].

II. INVESTIGATED MATERIAL

Nematogenic isotropic liquids are highly in demand materials for the Kerr effect [25–27]. These kinds of materials exhibit their nematic phases below their clearing points. Moreover, the clearing point should be slightly below room temperature, because within the temperature range of isotropic-nematic (*I-N*) phase transition, the material is very susceptible to external fields [11,13]. It consists of three two- and three-ring compounds (Table I). They were synthesized in the Institute of Chemistry, Military University of Technology, Warsaw, Poland. The first, polar compound (C1), has its melting point at 14 °C and monotropic-nematic phase at 6.8 °C [28]. This means a low temperature of the nematic-isotropic phase transition of the final NMHP mixture. The second (C2) and the third (C3) compounds are highly polar too. They entail liquid crystal behavior. The temperature range of the nematic phase is 95 °C for (C2) and 38 °C for (C3) [29]. Additionally, the last compound (C3) exhibits an additional liquid crystalline smectic-*C* phase in the temperature range over 22 °C. All compounds are fluorine (-F) substituted at their lateral positions. Values of the longitudinal components of the molecular dipole moments $\mu_{||}$ are about 8–10 D. Additionally, the molecular structures under study exhibit significant values of transverse dipole moments μ_{\perp} . Because of the double fluorine substitution at the C3

molecular core, the molecule is characterized by the highest value of μ_{\perp} , which is around 4 D, while in the case of the other two compounds (C1 and C2), it is close to 2 D.

In order to study the phase transition sequence of the NMHP compound, the bulk sample was investigated using the differential scanning calorimetry (DSC) method. DSC experiments were performed by a Netzsch DSC 204 F1 Phoenix instrument in an atmosphere of flowing nitrogen. Figure 1 indicates the first-order phase transition (exchange of heat) in the NMHP mixture upon heating and cooling cycles at a rate of 1.0 K/min. The *I-N* phase transition in the cooling cycle occurs at 18.5 °C, whereas in the heating cycle it occurs at 17.5 °C. Since the material is a three-component mixture, both observed peaks are broad. This is caused by the fact that the phase transition is more complicated than in a pure compound. Different molecules should adapt to each other. Therefore, the width of the phase

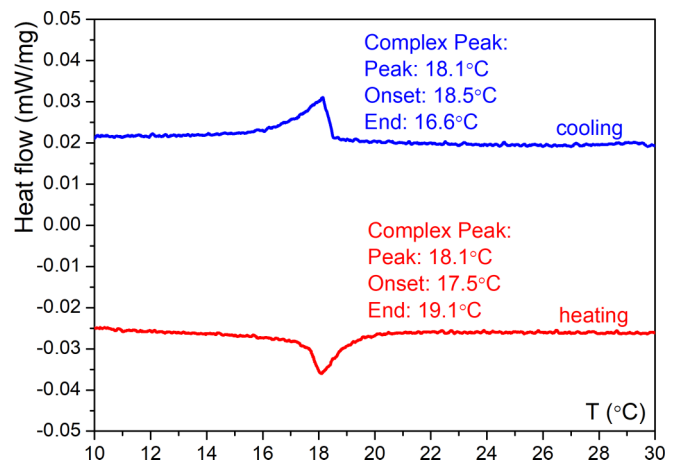


FIG. 1. DSC thermogram of the heating and cooling cycles obtained for the mixture under study.

transition is broad: At cooling it is 1.9°C while at heating it is 1.6°C. Usually multicomponent mixtures exhibit a wide phase transition. If the observed behavior were a result of phase separation, several peaks would be observed. The mixture does not have impurities because the low- and high-temperature sides of the peaks are almost straight lines.

III. EXPERIMENT

Measuring cells were filled by the NMHP mixture in the isotropic phase by capillary action. The custom-made cells were assembled from two float glass substrates. The inner surfaces of the cells were coated with unidirectionally rubbed SE 130 or SE 1211 (Nissan Chemicals) polyimides to obtain homogeneous (HG) and homeotropic (HT) alignment, respectively. This enables us to obtain ϵ_{\parallel} and ϵ_{\perp} permittivity tensor components in dielectric spectroscopy (DS) measurements. The DS measurements were performed by an impedance analyzer HP 4192A and conducted over a broad frequency range from 100 Hz to 10 MHz. Cells with low-resistivity indium tin oxide (ITO) electrodes with relatively low sheet resistivity ρ around 10 Ω per square (Ω/sq) and with gold electrodes ($\rho < 1 \Omega/\text{sq}$) were used. The disadvantage of using ordinary ITO electrodes ($\rho \approx 100 \Omega/\text{sq}$) is their too low cutoff frequency f_0 [30–34], which usually is around 200 kHz. For low-resistivity ITO, frequency is ca. 1 MHz, while for gold electrodes it is higher than 3 MHz. For planarly oriented cells (HG type) with ITO electrodes, the cell gap was 1.5 μm ; on the other hand, the thickness of the cells with gold electrodes (HT type) was 5.0 μm . The cells with the NMHP material under study were placed in a heating stage, Linkam THMSE600. The temperature was controlled by a Linkam TMS92 with an accuracy of 0.1 K. Data were collected every 0.5 K in a cooling cycle with a rate of 0.3 K/min. To cool samples below room temperature, dry ice was used. The impedance analyzer generated a bias (dc) electric field from 0 to 35 V. The measuring field (ac) was 0.1 V.

The order parameter, S , was calculated by using the guest-host system [22–24]. As a guest introduced into the NMHP material, a dichroic azo dye (AZO1 by Nematel Co. Ltd.) was chosen. Azo molecules have an elongated, rodlike molecular

shape. Based on the molecular structure, they are similar to a liquid crystal host which also contains rodlike molecules. The investigated NMHP mixture was doped with 1.0 wt% of the azo dye. Doping the mixture leads to an increase of the phase transition temperature by about 2°C. The sample was characterized by one maximum absorbance existing at approximately 487 nm. The absorption spectra were recorded by a charge-coupled device (CCD) spectrometer (Edmund Optics BRC 111A-USB-VIS-NIR) at a wave band from 340 to 770 nm. The order parameter, S , of the guest in the aligned sample was determined from the following equation [23,24]:

$$S = \frac{R - 1}{R + 2} = \frac{A_{\parallel} - A_{\perp}}{A_{\parallel} + 2A_{\perp}}, \quad (1)$$

where R is the dichroic ratio ($R = A_{\parallel}/A_{\perp}$) and A_{\parallel} and A_{\perp} are absorbance of the dye oriented parallel and perpendicular to the plane of polarization of an incident polarized light, respectively. The experiment aimed to obtain a value of the field-induced order parameter in the isotropic phase. For this reason, the electric field by a waveform generator Agilent 33220A gained with a voltage amplifier FLC Electronics F20A was applied to an IPS (in-plane switching) cell with a cell gap of 6 μm . A Linkam TMS93 hot stage controlled the sample temperature with accuracy not higher than 0.1 K.

IV. RESULTS AND DISCUSSION

The phase transition behavior of the investigated mesogenic mixture was confirmed using the polarizing optical microscope method (POM). Textures in Fig. 2 were taken in a 3- μm -thick cell under crossed polarizers during a cooling cycle. The phase transition between the isotropic and the nematic phase appears at 19.0°C [Fig. 2(b)]. The presented pictures reveal a biphasic region during the transition. The biphasic region (with a width of 2°C) is the result of the nematic phase formation process in the three-compound mixture. The width of the I - N transition corresponds to the first appearance of the bright nematic droplets [Fig. 2(b)] and disappearance of the dark isotropic state [Fig. 2(f)]. A similar phenomenon was observed during the DSC measurements.

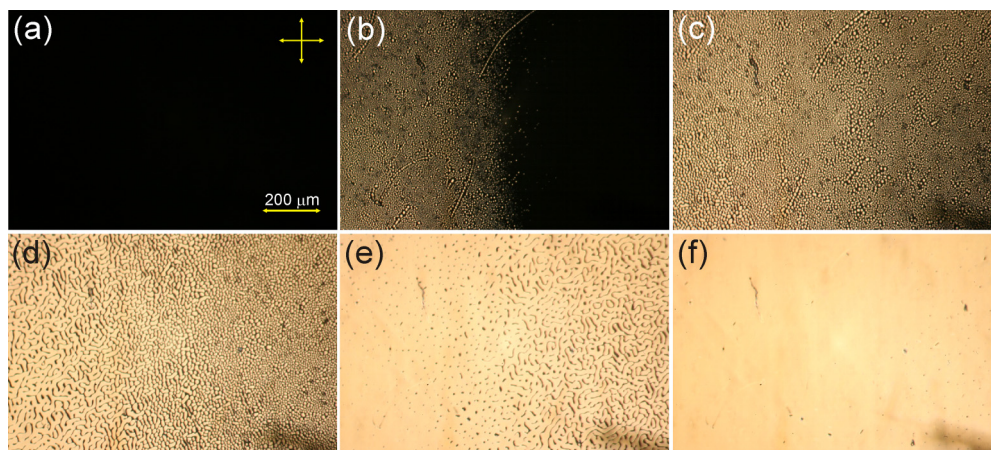


FIG. 2. The isotropic-nematic phase transition textures of the mesogenic mixture at (a) 19.5°C, (b) 19.0°C, (c) 18.5°C, (d) 18.0°C, (e) 17.5°C, and (f) 17.0°C.

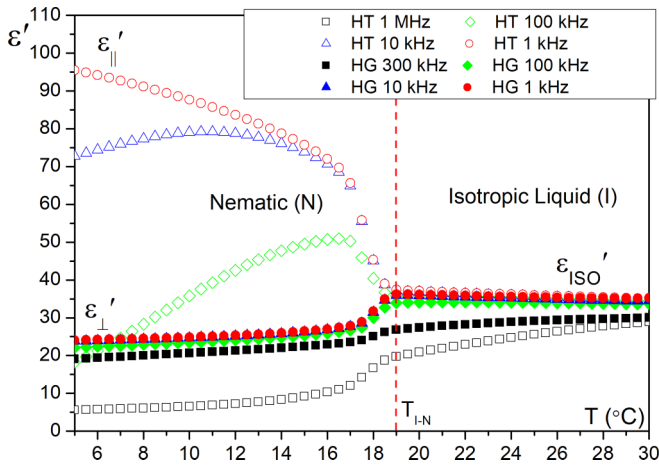


FIG. 3. The temperature dependence of real components of electric permittivity ϵ'_\parallel and ϵ'_\perp measured at several frequencies for NMHP. Phase transition temperature (T_{I-N}) between the isotropic and nematic phase is at 19°C.

Figure 3 presents the temperature dependence of a real part of electric permittivity ϵ' in the vicinity of the isotropic and the nematic phase of NMHP material. In the first step, DS measurements were done without the bias field. It was done to characterize basic material parameters, in particular the clearing temperature and the electric anisotropy in the nematic phase. Presented results show that at room temperature the investigated mixture exhibits the isotropic phase. The phase transition temperature between the *I* and *N* phases is at 19.0°C. The nematic phase is well built at 2°C below T_{I-N} . All experimental techniques used (DSC, POM, DS) confirm the creation of the nematic phase in the three-component mixture is a much more complex process than in one-compound liquid crystal materials. Similar behavior was previously observed for dual-frequency multicomponent mixtures [15]. In the nematic phase (at the temperature of 6°C), the material is characterized by large positive electric anisotropy which is equal to $\Delta\epsilon = 70.0$ at 1 kHz. It is worth underlining that values of electric permittivity measured in planar (HG) and homeotropic (HT) align-

ment are the same in the isotropic liquid. ϵ_I splits into ϵ_\parallel and ϵ_\perp exactly at the clearing temperature (T_{I-N}). Visible dispersion in the isotropic phase at a high-frequency region is connected by a molecular rotation around the principal axis of inertia (*S* mode) [35]. It is quite unusual because the *S* mode for many cyano compounds is observed at a couple hundred MHz or even at a frequency of a few GHz [35–38]. Additionally, in the nematic phase complex molecular relaxations are observed which may be attributed to the existence of the highly polar groups.

The dc electric field strongly interacts with the material in the isotropic phase. Figure 4 depicts the influence of the low [Fig. 4(a)] and high [Fig. 4(b)] bias field on the dielectric response. The results were obtained in two separate experiments. At the temperatures from 30°C to 28°C the material behaves typically [Fig. 4(a)]. We observe a gradual small increase of electric permittivity under the electric field. Further measurements show an unexpected decrease of electric permittivity in the isotropic phase. The electric bias field causes a shift of the *I-N* phase transition temperature toward the higher-temperature region, as was expected [39,40]. We assume that the creation of the field-induced nematic phase starts where the electric permittivity under the dc field starts growing from the level of ϵ for the zero-field isotropic liquid [Fig. 4(a)]. Therefore, at the electric field of 10 V per 1.5 μm , the clearing point was shifted upward by 1.0°C ($\delta T_{I-N} = 1.0^\circ\text{C}$). Under the influence of the higher bias field, the dielectric behavior of the NMHP material becomes much more complicated [Fig. 4(b)]. The decrease of the electric permittivity is still observed, but now in the whole temperature range of the isotropic phase. Moreover, near the phase transition, a single peak of electric permittivity is visible. The sharp increase of the electric permittivity occurs at about 2.5°C above the clearing temperature. A similar phenomenon was reported in our previous paper [16]. Now the phase transition temperature is shifted upward by 4.5°C (20 V per 1.5 μm). The decrease of ϵ is dependent on the bias field. For lower voltages, the decrease is much more pronounced than for higher ones. It seems that in the isotropic phase, at a strong bias field we could measure the values of electric permittivity close to those measured without a bias field. In the

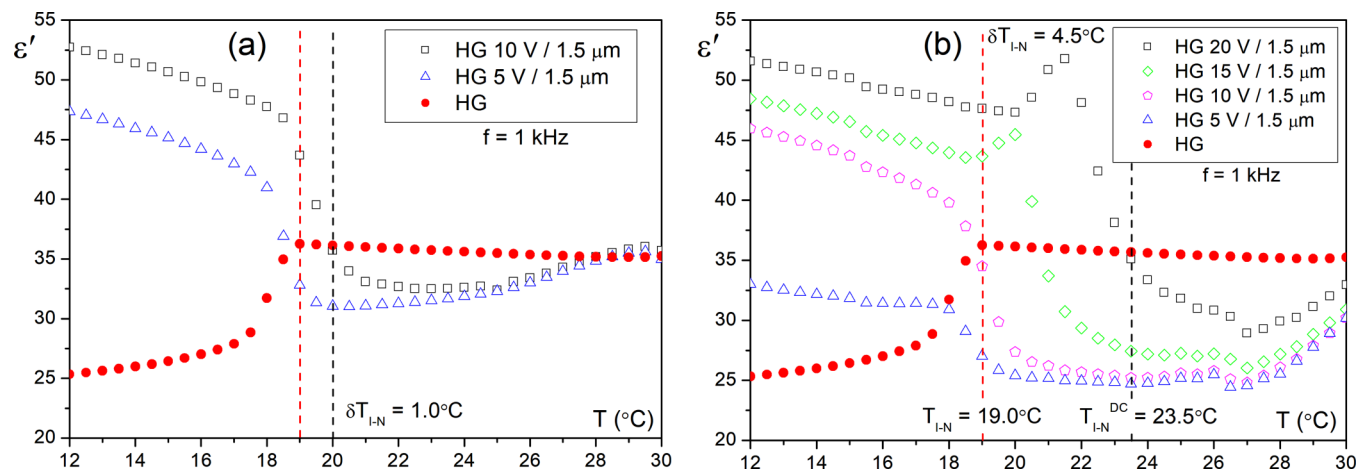


FIG. 4. Real part of electric permittivity ϵ' versus temperature T at frequency f of 1 kHz for the low- (a) and (b) high-bias electric fields. The red line marks the phase transition temperature T_{I-N} in measurements without the dc field. The black line marks the field-induced phase transition temperature T_{I-N}^{dc} under the highest electric field, which is shown in the figure.

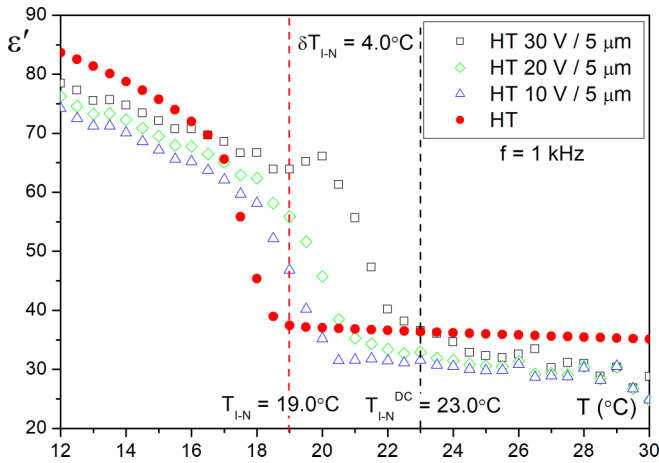


FIG. 5. Real part of electric permittivity ϵ' versus temperature T at frequency f of 1 kHz under different bias voltages. The red line marks the phase transition temperature T_{I-N} observed in measurements without the dc field, while the black line marks the field-induced phase transition temperature T_{I-N}^{DC} . Under the field of 30 V per 5 μm , the phase transition temperature shifted by 4.0°C.

nematic phase, the mixture behaves typically. However, when we compare values of ϵ'_{\parallel} measured in the homeotropically oriented cell (Fig. 3) and the planarly oriented cell with the bias field [Figs. 4(a) and 4(b)], we can notice the decrease of electric permittivity as well.

In the next step of the experiment, the bias electric field was applied to the homeotropically oriented cell with gold electrodes (Fig. 5). In the cell with the gold electrodes, we are able to observe high-frequency relaxations because the dispersion characteristics are not distorted up to 3 MHz (Fig. 6) due to the high cutoff frequency [30–34]. When using standard ITO electrodes, the frequency spectrum is limited to ca. 200 kHz. Therefore, it is impossible to determine relaxation parameters of molecular modes in the isotropic phase. Changing of electrodes did not affect the ion mobility.

The conducted experiment confirms previous behavior. The decrease of the electric permittivity in the isotropic phase was still observed. Moreover, now it is clearly visible that electric permittivity also diminishes in the nematic phase after applying the dc field (Fig. 5). The decrease of the electric permittivity in the isotropic and nematic phase still depends on the value of the bias voltage, as was previously seen in Figs. 4(a) and 4(b).

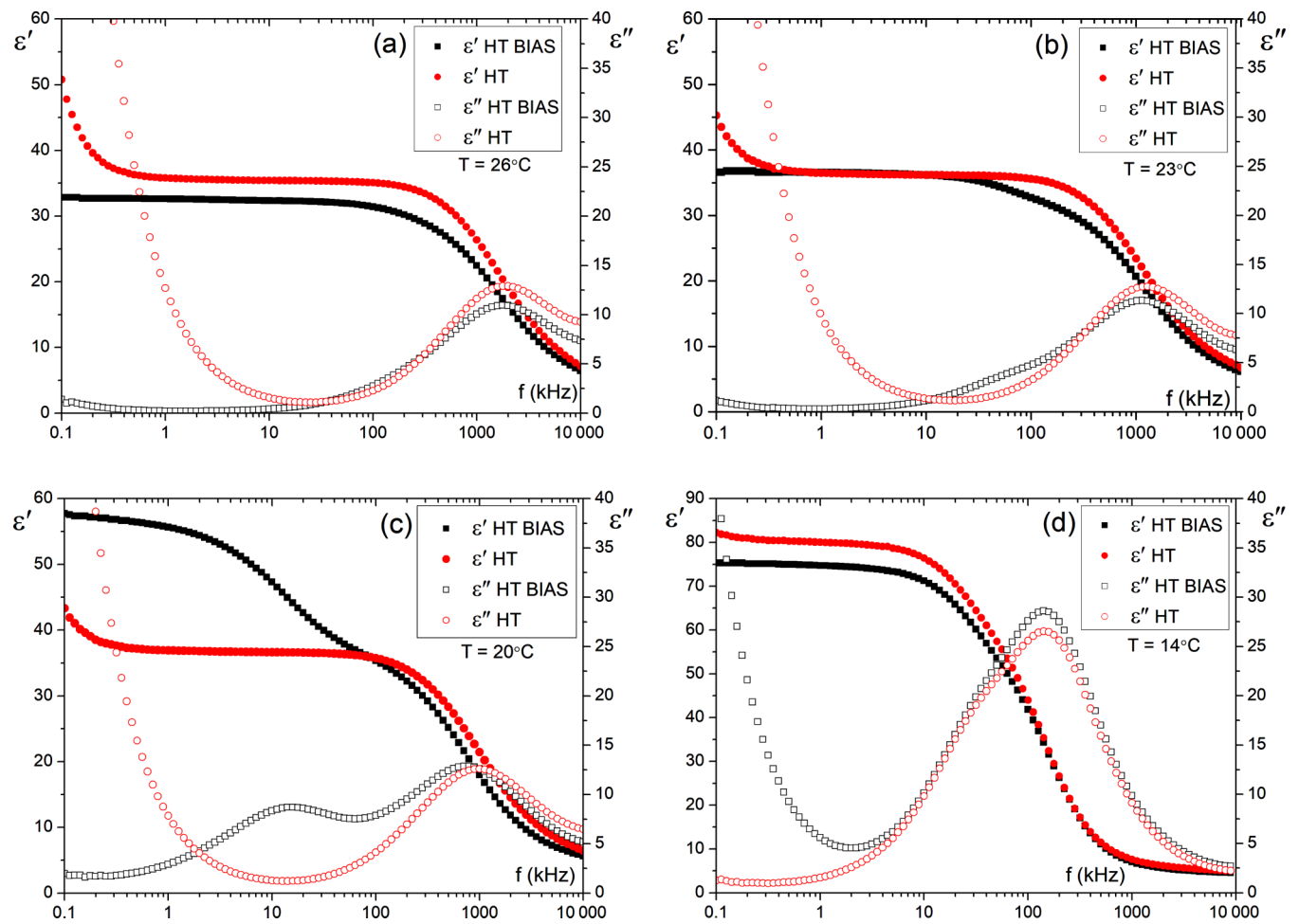


FIG. 6. Real (ϵ') and imaginary (ϵ'') parts of complex electric permittivity plotted against frequency (a) for the isotropic phase, (b) at the field-induced phase transition temperature, (c) at the temperature corresponding to the occurrence of the peak of electric permittivity, and (d) in the fully created nematic phase.

It is worth noting that the peak of electric permittivity in the homeotropic alignment appears for the bias field (30 V per 5 μm) at lower temperature than for the planar one (20 V per 1.5 μm). By applying 30 V per 5 μm , we can shift the phase transition temperature about 4.0 $^{\circ}\text{C}$.

Data from dielectric spectroscopy measurements with the gold electrodes were used to plot the dispersion and absorption spectra at specific temperatures. Figure 6 presents how the bias field influences molecular relaxation processes occurring in the whole phase sequence. In the isotropic phase [Fig. 6(a)] the electric field causes the appearance of two relaxation frequencies in the high-frequency region while without the bias field, only one relaxation is observed (rotation around short molecular axes). It seems that the field-induced relaxations are weaker than the zero-field molecular S mode. These two relaxations become more visible and stronger as temperature decreases [Fig. 6(b)]. They are strongest [Fig. 6(c)] in the temperature region where the peak of electric permittivity was noticed (Fig. 5). At 20 $^{\circ}\text{C}$ under the dc electric field, two strong well-separated modes are visible in the frequency domain. In contrast to the isotropic phase, in the nematic phase [Fig. 6(d)] two modes can be distinguished in the measurements with as well as without the bias field. It is worth mentioning here that under the bias field an ion current is stopped since the imaginary part of electric permittivity diminishes for low frequencies up to 10 kHz. This effect appears because the bias field traps ions on the electrodes' surfaces. Consequently, the ions' mobility decreases.

In order to fully understand the dielectric response of NMHP material in the electric field, the relaxation parameters were calculated using the numerical procedure reported elsewhere [30–32]. The numerical procedure is based on the Cole-Cole model [41]. The Cole-Cole model is a modified version of the Debye model [42] which is often used in research on liquid crystal materials to describe a single molecular relaxation. In contrast, The Cole-Cole model introduces into the Debye model the distribution parameter, α , as follows:

$$\varepsilon^*(f) = \varepsilon_{\infty} + \frac{\delta\varepsilon}{1 + (j\frac{f}{f_R})^{1-\alpha}}, \quad (2)$$

where f_R is the relaxation frequency, $\delta\varepsilon$ is the dielectric strength, and ε_{∞} is the high-frequency limit of electric permittivity. If α is equal to zero then the Debye model is applied [41]. A relaxation process is a single molecular rotation with a single, well-defined relaxation frequency. For $\alpha > 0$ the Debye model transforms into the Cole-Cole model [42]. Thus, the dispersion is observed in a wider range of frequencies. Besides this, the model allows us to find the relaxation frequency, where the imaginary part of electric permittivity ε'' represents the maximum value. Also, f_R is referred to as an inflection point on a dispersion spectrum. The relaxation frequency describes dynamic properties of a liquid crystal under an electric field. Above the relaxation frequency, the contribution of a mode to the dielectric response begins to decrease. The dielectric strength of a mode is the difference between the static electric permittivity ε_S (determined for low frequencies $f \rightarrow 0$) and the optical electric permittivity ε_{∞} (determined for high frequencies $f \rightarrow \infty$).

In the numerical procedure, the electric permittivity $\varepsilon_{\text{expt}}$, known from the experiment, is compared to the effective electric permittivity ε_{ef} , calculated from the model [30]. The

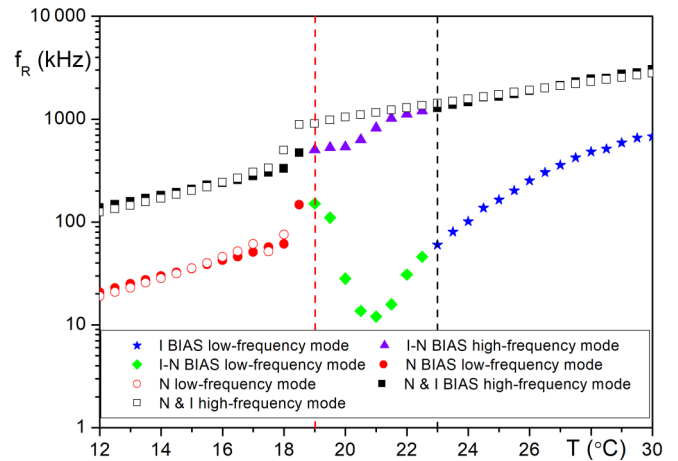


FIG. 7. Calculated values of the relaxation frequency f_R versus temperature T in the vicinity of the isotropic (I) and nematic phase (N). The filled symbols mark results for the measurements with the bias field (BIAS), which equals to 30 V. Field-induced phase transition temperature is 23 $^{\circ}\text{C}$. Field-free phase transition temperature is 19 $^{\circ}\text{C}$. Here, abbreviation I - N stands for the field-induced phase transition region, while N and I indicate the presence of the same mode in the isotropic and the nematic phase. The red line marks the field-free phase transition, while the black line marks the field-induced phase transition temperature.

effective electric permittivity takes into account the cutoff frequency f_0 [31] and the resonance frequency f_{RE} [30] which strongly influence measurements in the high-frequency region as parasitic effects. Moreover, in the formulas for the effective electric permittivity, the part related to ion currents is also considered. The optimization method, working on the principle of feedback, fits the experimental results together with the effective results. The proper values of the all parameters (f_R , $\delta\varepsilon$, α , ε_{∞}) of visible modes are found when the discrepancy between $\varepsilon_{\text{expt}}$ and ε_{ef} is minimal. In the following paragraphs, we compare the relaxation parameters of the molecular modes in the measurements with and without the bias electric field.

Figure 7 depicts the relaxation frequency upon reaching the temperature in the vicinity of the isotropic and nematic phase transitions. Without the bias field, all the relaxation frequencies decrease as the temperature decreases. In the nematic phase, we observe low- (red open circles) and high-frequency (black open squares) relaxations, while in the isotropic phase only the one relaxation can be distinguished. High-frequency relaxation in the nematic phase is a continuation of the molecular mode which exists in the isotropic liquid. Under the influence of the dc field in the isotropic liquid, an additional low-frequency relaxation appears (blue filled stars), which f_R changes very quickly. Relaxation frequency drops from 680 kHz at 30 $^{\circ}\text{C}$ to 60 kHz at 23 $^{\circ}\text{C}$. In measurements with the bias field, the relaxation frequencies of the high-frequency relaxation (black filled squares) overlap completely in the N phase and partially in the I phase. On the one hand, near the field-induced phase transition region (19 $^{\circ}\text{C}$ –22.5 $^{\circ}\text{C}$) the f_R parameter of the high-frequency relaxation (violet filled triangles) decreases from around 1 MHz to 500 kHz. On the other hand, the

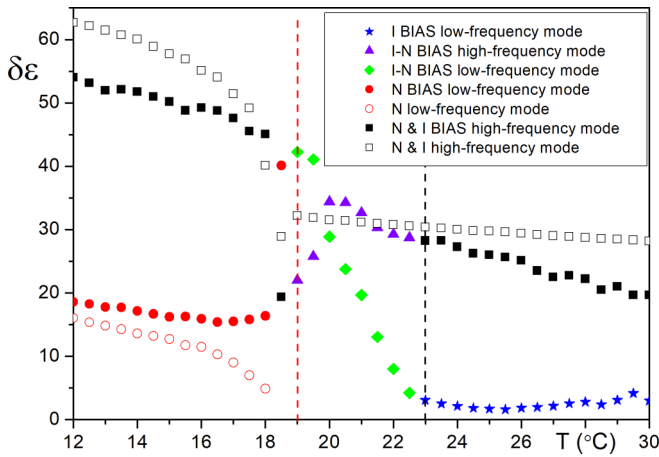


FIG. 8. Dielectric strength $\delta\epsilon$ of the high- and low-frequency relaxations upon temperature T in the vicinity of the isotropic (I) and nematic phase (N). The filled symbols mark results for the measurements with the bias field (BIAS), which equals to 30 V. Field-induced phase transition temperature is 23 °C. Field-free phase transition temperature is 19 °C. Here, abbreviation I - N stands for the field-induced phase transition region, while N and I indicate the presence of the same mode in the isotropic and the nematic phase. The red line marks the field-free phase transition, while the black line marks the field-induced phase transition temperature.

low-frequency relaxation frequency starts growing rapidly from around 10 to 150 kHz (green filled diamonds).

Under the bias electric field, the dielectric strength of the high-frequency relaxation in the whole temperature range is weaker than the one observed without the dc field (Fig. 8). Moreover, in the nematic phase, the low-frequency relaxation under the electric field (red filled squares) has a higher value of $\delta\epsilon$ than the relaxation process in the measurements without the bias electric field (red open squares). We can notice that the field-induced low-frequency mode in the isotropic liquid (blue filled stars) is poorly detectable. However, this mode becomes very strong at the phase transition region (green filled diamonds), where a sharp increase of electric permittivity is observed. In contrast, the dielectric strength of the high-frequency relaxation (violet filled triangles) diminishes at the same time.

Detailed results on the distribution parameter are presented in Fig. 9. In the absence of the electric field, we observe that in the isotropic liquid phase of the NMHP material the high-frequency mode (black open squares) is characterized by the larger distribution parameter than in the nematic phase. Furthermore, in the nematic phase, the low-frequency relaxation (red open circles) can be regarded as the pure Debye mode. Parameter α is almost equal to zero. Under these circumstances, we can assume that all modes observed in the nematic phase are single-molecular rotations around short molecular axes, because of their low distribution parameters. In the field-driven isotropic-nematic phase transition, the situation is much more complicated, as was observed for relaxation frequency and dielectric strength results (Figs. 7 and 8). Here, in the high-temperature region (23 °C–30 °C), the distribution parameter (black filled squares) increases from 0.10 to 0.17 while temperature decreases. Values of α for the

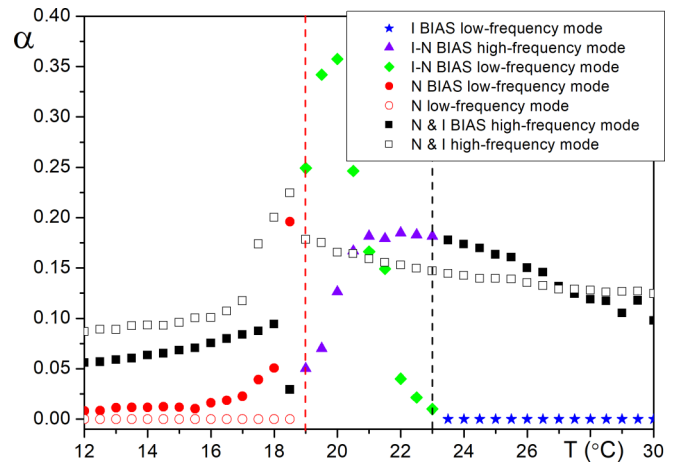


FIG. 9. Distribution parameter α in the Cole-Cole model versus temperature (T) in the vicinity of the isotropic (I) and the nematic (N) phases. The filled symbols mark results for the measurements with the bias field (BIAS), which equals to 30 V. Field-induced phase transition temperature is 23 °C. Field-free phase transition temperature is 19 °C. Here, the abbreviation I - N stands for the field-induced phase transition region, while N and I indicate the presence of the same mode in the isotropic and the nematic phases. The red line marks the field-free phase transition, while the black line marks the field-induced phase transition temperature.

field-induced low-frequency mode (blue filled stars) are rather constant (around 0). In the field-driven phase transition, the distribution parameter for the high-frequency mode (violet filled triangles) suddenly decreases almost to 0, in contrast to low-frequency relaxation (green filled diamonds) where the increase of α was detected. The value is highest at 19.5 °C, near the temperature corresponding to the occurrence of the peak of electric permittivity (20.0 °C). The distribution parameter increases from 0.01 (23 °C) to 0.36 (20 °C).

The field-induced order parameter S of the isotropic liquid crystal mixture was calculated in the guest-host system. Figure 10 depicts the reduced temperature dependence of the order parameter S . The measurements confirm the creation of the nematic order in the isotropic liquid after applying the electric field. The shift of the phase transition temperature observed during dielectric spectroscopy investigations means that we observe a significant increase of the order parameter in the isotropic phase of NMHP material. At the phase transition temperature T_{I-N} , where the phase is very susceptible to external forces, the field-induced order parameter reaches 0.30. This means that the orientational order is similar to that which is observed for the fully created nematic phase. As temperature decreases the field-induced order parameter S increases. This parameter becomes constant and low (~ 0.05) in the measurements without the electric field, as expected in the isotropic liquid. Furthermore, during the experiment, it was easy to switch between the isotropic and anisotropic phase by using the electric field.

In the presented experimental results two phenomena were described. Firstly, the values of electric permittivity in the isotropic phase decrease after application of the electric field. In most cases, the situation is reversed because the electric field creates a nematic molecular order within the isotropic phase.

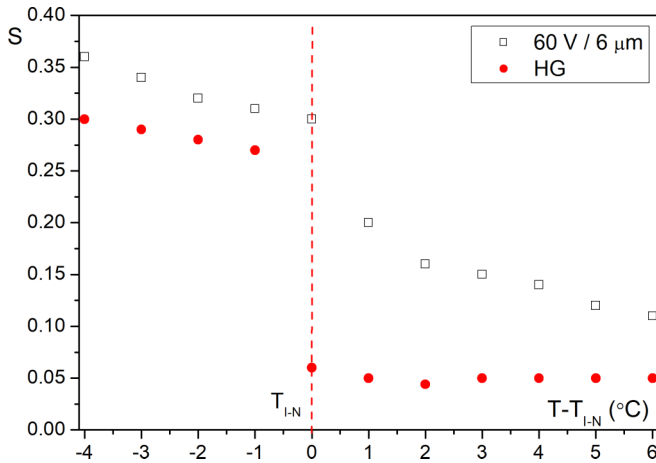


FIG. 10. Field-free and electric field-induced order parameter (S) of the highly polar nematogenic mixture upon the reduced temperature $T - T_{I-N}$. The order parameter was calculated using a dichroic ratio of the azo dye molecule in the guest-host system. Measurements were taken in the vicinity of the isotropic and nematic phase transition without (HG) and after applying the electric field (60 V per $6 \mu\text{m}$).

For this reason, the measured electric permittivity with the strong bias field during dielectric spectroscopy measurements is higher than for the pure isotropic phase. Secondly, in the field-induced phase transition region, the electric permittivity increases significantly at a specific temperature. The occurrence of the peak of the electric permittivity is related to the sudden change of relaxation parameters.

A possible explanation for the occurring phenomena is the field-induced creation of some complex molecular objects [Fig. 11(a)]. For the decrease of electric permittivity in the isotropic phase as well as in the nematic phase of the investigated mixture, quadrupoles seem to be responsible [Fig. 11(b)]. Quadrupoles consist of pairs of antiparallel dipoles. Hence, the total charge and total dipole moment of these objects are close to zero. Under the homogeneous electric field, molecular dipoles trapped in such quadrupoles do not rotate and do

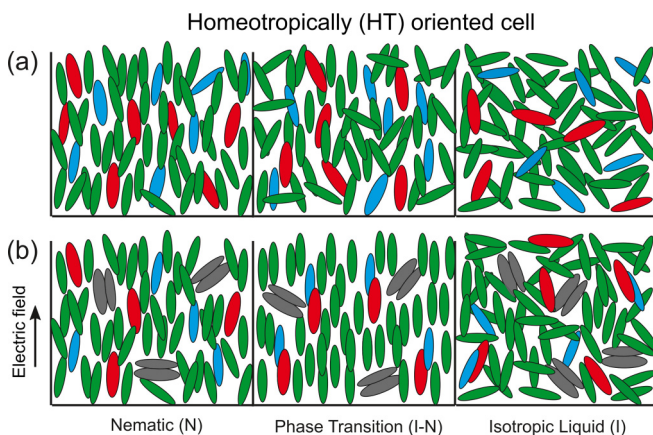


FIG. 11. Phase transition from the isotropic to the nematic phase in the investigated mixture in the homeotropically oriented cell (a) without the external field, and (a) with electric bias field. In green are the C1 molecules, while in blue and red are the C2 and C3 molecules, respectively. The quadrupoles are marked in gray.

not move (dipoles in such quadrupoles cancel their dipole moments); therefore, they do not give any contribution to the dielectric response. As a consequence, quadrupoles reduce the value of the dielectric constant. Why is the decrease much more pronounced for the lower dc voltages? We assume that just after applying the low bias voltage the quadrupoles are created. Applying increasing voltages causes the gradual disappearance of these objects. The force of electrostatic attraction between two dipole moments in the created quadrupoles is probably weak. With the increase of the external electric field, the distance between the dipole moments is increased resulting in the disappearance of the quadrupoles. Furthermore, some quadrupoles can change into dimers (two molecules which do not cancel their dipole moments). When the applied field is high enough, it is possible to observe the material where no quadrupoles exist under the external field.

In contrast, dimers may be responsible for the appearance of low-frequency relaxation in the isotropic liquid and the field-driven phase transition region [Fig. 8(b)], whereas the high-frequency relaxation comes from the S mode of the C1 molecule. This relaxation is weaker in the field-induced isotropic phase because of the influence of quadrupoles or rather the competition between dimers and quadrupoles. Regarding dimers, their share in volume gets bigger and bigger as temperature decreases. Most of the molecules create the dimers at the temperature corresponding to the occurrence of the peak of electric permittivity because the low-frequency relaxation becomes very strong and $\delta\epsilon$ of the high-frequency mode suddenly diminishes. At the edge of the nematic phase, they are aligned along the field due to the high-order parameter. A similar phenomenon was observed previously [16]. In the nematic phase, the dimerization process disappears, while in measurements with and without the dc field we observe two modes with almost the same relaxation frequencies. However, with the dc field, the low-frequency relaxation is a little stronger and possesses a slightly higher α parameter because a small share of dimers still exists in the nematic medium. As for the isotropic liquid, the high-frequency mode comes from the C1 molecules. The relaxation in the lower-frequency region of the nematic phase is connected with the S mode of the C2 and C3 compounds.

V. CONCLUSIONS

We reported here the decrease of the electric permittivity in the isotropic and the nematic phases under the bias of an electric field. Most likely the effect was caused by the field-induced creation of quadrupoles. The electric field also causes the creation of dimers. The low-frequency relaxation manifests the occurrence of dimers in the dielectric response. The dimers are responsible for the appearance of the peak of the electric permittivity near the clearing point, where the sudden change of the parameters of the molecular relaxations was observed. The presented results are experimental evidence that the created complex molecular objects cause a significant enhancement of the field-induced order parameter and a sharp increase of electric permittivity in the polar mesogenic mixture under study.

In the investigated mixture we can easily create the anisotropic material from the isotropic one. Due to this unique property, the mesogenic mixture is a very promising material for nonlinear devices based on the Kerr effect. The material

can be useful in applications for isotropic liquid crystal displays because of the potential of a low driving voltage and significant field-induced birefringence, which is not discussed here but one can realize that the creation of the anisotropic phase in an isotropic liquid should generate birefringence.

ACKNOWLEDGMENTS

The authors would like to thank Carol Grzych for constructive criticism of the manuscript. This work was supported by Military University of Technology Grants No. PBS 23-652 and No. RMN 08-792.

-
- [1] Y.-C. Yang and D.-K. Yang, *Appl. Phys. Lett.* **98**, 023502 (2011).
- [2] M. J. Bradshaw and E. P. Raynes, *Mol. Cryst. Liq. Cryst.* **72**, 73 (1981).
- [3] T. Ostapenko, D. B. Wiant, S. N. Sprunt, A. Jáklí, and J. T. Gleeson, *Phys. Rev. Lett.* **101**, 247801 (2008).
- [4] A. Drozd-Rzoska, S. J. Rzoska, and J. Ziolo, *J. Phys.: Condens. Matter* **12**, 6135 (2000).
- [5] S. J. Rzoska, S. Starzonek, A. Drozd-Rzoska, K. Czupryński, K. Chmiel, G. Gaura, A. Michulec, B. Szczypek, and W. Walas, *Phys. Rev. E* **93**, 020701(R) (2016).
- [6] A. Drozd-Rzoska, S. Pawlus, and S. J. Rzoska, *Phys. Rev. E* **64**, 051701 (2001).
- [7] M. Janik, S. J. Rzoska, A. Drozd-Rzoska, J. Ziolo, P. Janik, S. Maślanka, and K. Czupryński, *J. Chem. Phys.* **124**, 144907 (2006).
- [8] J. Jadżyn and G. Czechowski, *Opto-Electron. Rev.* **16**, 395 (2008).
- [9] T. W. Stinson and J. D. Litster, *Phys. Rev. Lett.* **25**, 503 (1970).
- [10] Y. Kawata, H. Yoshida, S. Tanaka, A. Konkanok, M. Ozaki, and H. Kikuchi, *Phys. Rev. E* **91**, 022503 (2015).
- [11] P. G. de Gennes and J. Prost, *The Physics of Liquid Crystals*, 2nd ed. (Clarendon Press, Oxford, 1995).
- [12] P. Oswald and P. Pieranski, *Nematic and Cholesteric Liquid Crystals: Concepts and Physical Properties Illustrated by Experiments*, 1st ed. (CRC Press, Boca Raton, FL, 2005).
- [13] F. Costache and M. Blasl, *Opt. Photonik* **6**, 29 (2011).
- [14] M. Schadt and W. Helfrich, *Mol. Cryst. Liq. Cryst.* **17**, 355 (1972).
- [15] M. Mrukiewicz, P. Perkowski, K. Garbat, and R. Dąbrowski, *Liq. Cryst.* **41**, 1537 (2014).
- [16] M. Mrukiewicz, P. Perkowski, R. Mazur, O. Chojnowska, W. Piecek, and R. Dąbrowski, *J. Mol. Liq.* **223**, 873 (2016).
- [17] E. Wolarz, D. Bauman, J. Jadżyn, and R. Dąbrowski, *Acta Phys. Pol., A* **120**, 447 (2011).
- [18] A. Drozd-Rzoska, S. J. Rzoska, J. Ziolo, and J. Jadżyn, *Phys. Rev. E* **63**, 052701 (2001).
- [19] G. Vertogen and W. H. de Jeu, *Thermotropic Liquid Crystals, Fundamentals* (Springer, Berlin, 1988).
- [20] M. A. Anisimov, *Critical Phenomena in Liquids and Liquid Crystals* (Gordon and Breach, Philadelphia, 1991).
- [21] D. Ganzke, S. Wróbel, and W. Haase, *Mol. Cryst. Liq. Cryst.* **409**, 323 (2004).
- [22] H. Ichinose, H. Sato, and S. Naemura, *Mol. Cryst. Liq. Cryst.* **409**, 401 (2004).
- [23] D. Bauman and H. Moryson, *J. Mol. Struct.* **404**, 113 (1997).
- [24] M. T. Sims, L. C. Abbott, S. J. Cowling, J. W. Goodby, and J. N. Moore, *Chemistry* **21**, 10123 (2015).
- [25] J. C. Filippini and Y. Poggi, *J. Phys. D: Appl. Phys.* **8**, L152 (1975).
- [26] Y. Haseba and H. Kikuchi, *J. Soc. Inf. Disp.* **14**, 551 (2006).
- [27] B.-X. Li, V. Borshch, S. V. Shiyonovskii, S.-B. Liu, and O. D. Lavrentovich, *Phys. Rev. E* **92**, 050501 (2015).
- [28] M. Sasaki, K. Takeuchi, H. Sat[obar], and H. Takatsu, *Mol. Cryst. Liq. Cryst.* **109**, 169 (1984).
- [29] D. Ziobro, P. Kula, J. Dziaduszek, M. Filipowicz, R. Dąbrowski, J. Parka, J. Czub, S. Urban, and S. T. Wu, *Opto-Electron. Rev.* **17**, 16 (2009).
- [30] P. Perkowski, *Opto-Electron. Rev.* **20**, 79 (2012).
- [31] P. Perkowski, *Opto-Electron. Rev.* **19**, 176 (2011).
- [32] Perkowski, *Opto-Electron. Rev.* **19**, 76 (2011).
- [33] P. Perkowski, *Phase Trans.* **83**, 836 (2010).
- [34] P. Perkowski, *Opto-Electron. Rev.* **17**, 180 (2009).
- [35] W. Haase and S. Wróbel, *Relaxation Phenomena: Liquid Crystals, Magnetic Systems, Polymers, High-Tc Superconductors, Metallic Glasses* (Springer Science & Business Media, Berlin, 2013).
- [36] J. Jadżyn, L. Hellemans, G. Czechowski, C. Legrand, and R. Douali, *Liq. Cryst.* **27**, 613 (2000).
- [37] J. Czub, R. Dąbrowski, S. Urban, and D. Ziobro, *Z. Naturforsch., J: Phys. Sci.* **65**, 221 (2010).
- [38] J. Czub, S. Urban, D. Ziobro, and R. Dąbrowski, *Mol. Cryst. Liq. Cryst.* **508**, 286/[648] (2009).
- [39] E. I. Rjuntse, M. A. Osipov, T. A. Rotinyan, and N. P. Yevlampieva, *Liq. Cryst.* **18**, 87 (1995).
- [40] W. Helfrich, *Phys. Rev. Lett.* **24**, 201 (1970).
- [41] P. Debye, *Verh. Dtsch. Phys. Ges.* **15**, 777 (1913).
- [42] K. S. Cole and R. H. Cole, *J. Chem. Phys.* **9**, 341 (1941).